Ionics (2008) 14:441–447
DOI 10.1007/s11581-007-0195-7

ORIGINAL PAPER

Pseudo-capacitive properties of $LiCoO_2$/AC electrochemical capacitor in various aqueous electrolytes

Lian-Mei Chen · Qiong-Yu Lai · Yan-Jing Hao · Jian-hua huang · Xiao-Yang Ji

Received: 25 September 2007 / Revised: 17 November 2007 / Accepted: 3 December 2007 / Published online: 5 January 2008

Abstract $LiCoO_2$ particles were synthesized by a sol-gel process. X-ray diffraction analysis reveals that the prepared sample is a single phase with layered structure. A hybrid electrochemical capacitor was fabricated with $LiCoO_2$ as a positive electrode and activated carbon (AC) as a negative electrode in various aqueous electrolytes. Pseudo-capacitive properties of the $LiCoO_2$/AC electrochemical capacitor were determined by cyclic voltammetry, charge–discharge test, and electrochemical impedance measurement. The charge storage mechanism of the $LiCoO_2$-positive electrode in aqueous electrolyte was discussed, too. The results showed that the potential range, scan rate, species of aqueous electrolyte, and current density had great effect on capacitive properties of the hybrid capacitor. In the potential range of 0–1.4 V, it delivered a discharge specific capacitance of 45.9 Fg^{-1} (based on the active mass of the two electrodes) at a current density of 100 mAg^{-1} in 1 $molL^{-1}$ Li_2SO_4 aqueous electrolyte. The specific capacitance remained 41.7 Fg^{-1} after 600 cycles.

L.-M. Chen · Q.-Y. Lai (✉) · Y.-J. Hao · J.-h. huang
College of Chemistry, Sichuan University,
Chengdu 610064, People's Republic of China
e-mail: Laiqy5@hotmail.com

L.-M. Chen
College of Chemistry and Chemical Engineering,
China West Normal University,
Nanchong,
Sichuan 637000, People's Republic of China

X.-Y. Ji
Analyzing and Testing Center, Sichuan University,
Chengdu 610064, People's Republic of China

Keywords Electrochemical capacitor · $LiCoO_2$ · Sol-gel process · Electrochemical measurements · Pseudo-capacitive properties

Introduction

Electrochemical capacitors, also named as supercapacitors, have attracted special attention due to their potential applications in many fields such as hybrid electric vehicles, electronic devices, and memory back-up systems [1]. On the basis of the charge storage mechanisms, there are two major categories: electric double-layer capacitors (EDLCs) and pseudo-capacitors. EDLCs employ various kinds of carbon as electrode materials, which utilize the double-layer capacitance arising from the charge separation at an electrode–electrolyte interface. Pseudo-capacitors use transition metal oxides or conducting polymers as electrode materials, which utilize the charge-transfer pseudo-capacitance arising from the fast and reversible Faradaic reactions occurring in the electrode. Among these electrode materials, amorphous hydrous ruthenium oxide (RuO_2xH_2O) exhibits ideal pseudo-capacitive behavior with large specific capacitance and great reversibility [2–4], but it is too expensive to be commercially attractive. Therefore, many efforts are made to search for alternative materials such as MnO_2, NiO, CoO_x, and V_2O_5 [5–11].

Recently, there are some reports on lithium insertion compounds (such as $Li_4Ti_5O_{12}$, $Li_2Ti_3O_7$, and $LiCoO_2$/AC composite) used as the electrode materials of supercapacitors in organic electrolyte [12–15]. It is found that $LiCoO_2$ can exhibit good pseudo-capacitive properties in aqueous electrolyte, too. As compared to organic electrolyte, aqueous electrolyte has many advantages (e.g., high ionic conductivity, low cost, good safe character, etc.). Therefore, in

present work, pseudo-capacitive properties of $LiCoO_2$ were investigated in Li^+, Na^+, K^+, and NH_4^+ aqueous solution, respectively; the charge storage mechanism of $LiCoO_2$ in aqueous electrolyte was also discussed. The work has not been reported to our best knowledge.

Experimental

Preparation of $LiCoO_2$

The $LiCoO_2$ particles were synthesized by a sol-gel process. Required amount of $Li(CH_3COO)_2 2H_2O$ (AR) and $Co(CH_3COO)_2 4H_2O$ (AR) was dissolved in distilled water with the molar ratio of Li/Co=1.02:1 and then certain amount of citric acid was added to this solution to chelate metal ions at 60 °C under water bath with constantly stirring. Aqueous ammonia was added slowly to this mixture solution until the pH value of 5 was achieved. The obtained solution was heated to 90 °C and then certain amount of glycol was added. This last solution was heated at 90 °C until a gel formed. The resulting gel was dried at 110 °C under vacuum to extract out excessive water and yielded a dry puffy precursor. The gel precursor was preheated at 400 °C in air for 3 h to decompose the organic components and further calcined at 800 °C for 10 h to obtain final product.

Characterization of the sample

Powder X-ray diffraction (XRD) data were collected on a Rigaku D/MAX–rA diffractometer with CuKα radiation, operating at 40 kV and 100 mA.

Electrochemical measurement

The $LiCoO_2$ electrode was prepared by mixing 70 wt.% $LiCoO_2$ powders, 25 wt.% acetylene black, and 5 wt.% polyvinylidene fluoride (PVDF) as a binder. The mixture was pressed onto stainless steel grids and then dried for 24 h at 65 °C under vacuum. The preparation procedures of the AC electrode were similar to that of the $LiCoO_2$ electrode. The ratio of AC, acetylene black, and PVDF was 65:30:5 (wt.%). All electrochemical tests were carried out at room temperature in aqueous solutions.

The cyclic voltammetry test was performed with a three-electrode cell in which platinum foil and saturated calomel electrode (SCE) were used as the counter and the reference electrode in 1 $molL^{-1}$ Li_2SO_4 solution, and it was carried out with LK2005 electrochemical workstation system.

The charge–discharge test was performed with a two-electrode cell in which the $LiCoO_2$ and AC electrode were respectively used as the positive and negative electrode in 1 $molL^{-1}$ Li_2SO_4, Na_2SO_4, K_2SO_4, and $(NH_4)_2SO_4$ solution, and it was carried out with Neware battery program-control testing system.

Electrochemical impedance spectroscopy (EIS) was measured in a three-electrode cell equipped with the working electrode, a platinum foil counter electrode, and an SCE; it was performed by Potentiostat Galvanostat PGSTAT302 (Netherlands) in 1 $molL^{-1}$ Li_2SO_4, Na_2SO_4, K_2SO_4, and $(NH_4)_2SO_4$ solution.

Results and discussion

XRD analysis

Figure 1 shows the X-ray diffraction pattern of the prepared $LiCoO_2$ sample. As can be seen in Fig. 1, all diffraction peaks are in agreement with JCPDS file (JCPDS card no. 16-0427), indicating that the prepared $LiCoO_2$ is a single phase. In the XRD pattern, the intensity ratio of (003) and (104) is 2.8, which is similar to the ratio in JCPDS file. Peak splitting clearly appears between (018) and (110) peaks and between (006) and (012) peaks. These data reveal that the as-prepared $LiCoO_2$ has a well-developed layered structure [16, 17].

Electrochemical analysis

Cyclic voltammetry analysis

Potential range is one of the predominant factors influencing the capacitive properties of supercapacitor. Generally, the broader the potential range is, the higher the energy density of the supercapacitor is. Hence, the potential range is controlled in the largest range in order to obtain the highest energy density under the condition that the electrode material

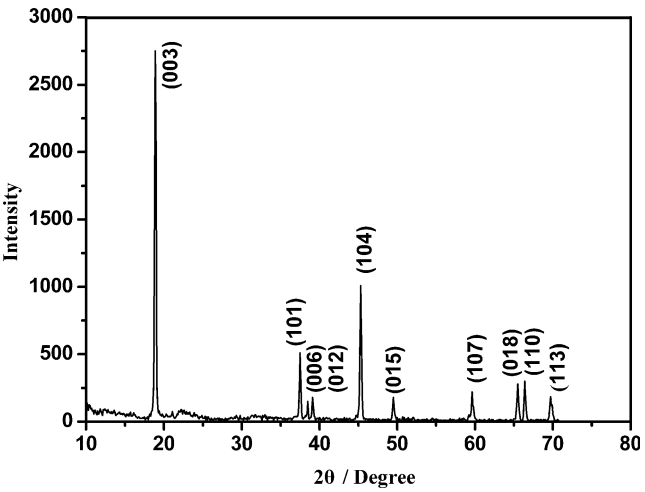

Fig. 1 XRD pattern of the prepared $LiCoO_2$ sample

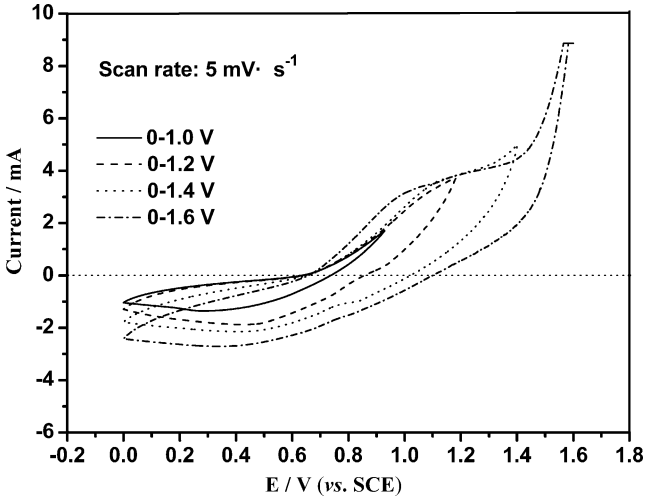

Fig. 2 CV curves of the $LiCoO_2$ electrode in various potential ranges in 1 $molL^{-1}$ Li_2SO_4

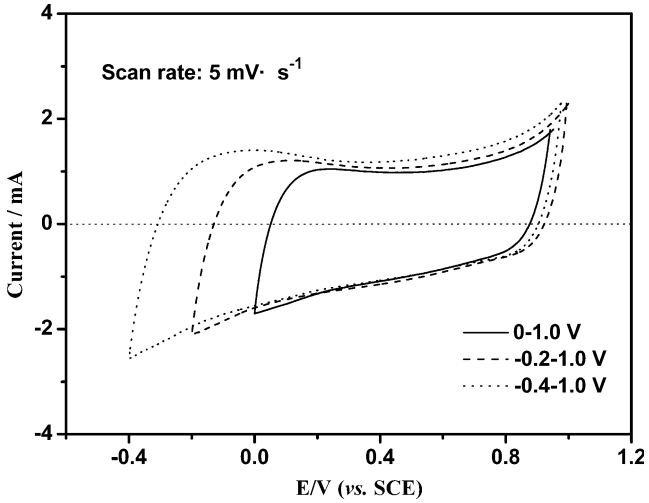

Fig. 4 CV curves of the AC electrode in various potential ranges in 1 $molL^{-1}$ Li_2SO_4

and electrolyte remain stable. To guarantee that the electrolyte will not decompose during charge–discharge process in aqueous system, it is important to control a safe potential window without O_2 and H_2 evolution on the surface of the electrodes.

Figure 2 shows the cyclic voltammogram (CV) curves of the $LiCoO_2$ electrode in various potential ranges at a scan rate of 5 mVs^{-1} in 1 $molL^{-1}$ Li_2SO_4. As can be seen in the figure, the O_2 evolution occurs when the voltage value is over 1.4 V (vs. SCE); it does not occur at the voltage value of 1.4 V (vs. SCE), which is higher than the potential of O_2 evolution (about 1.2 V vs. normal hydrogen electrode). We speculate that there is a high over-potential of O_2 evolution on the surface of $LiCoO_2$. Thus, the safe potential window for $LiCoO_2$ material is controlled between 0 and 1.4 V in 1 $molL^{-1}$ Li_2SO_4. From the CV curves of $LiCoO_2$ in the potential range of 0–1.4 V, a pair of broad redox peaks located at about 0.5 and 1.0 V (vs. SCE) is observed. When changing the potential scanning direction, the current direction does not turn around instantly, indicating that the insertion–extraction of Li-ions occurs not only on the surface of the $LiCoO_2$ powders but also into the inner lattice of the material. The diffusion rate of Li-ions is much lower in the inner lattice of the material than on the surface of the material, so it leads to slower current response.

Figure 3 shows the CV curves of the $LiCoO_2$ electrode at various scan rates in 1 $molL^{-1}$ Li_2SO_4 aqueous solution. When the scan rate is below 20 mVs^{-1}, it is observed that there appears a pair of redox peaks in the CV curves, suggesting Li-ions could diffuse into the inner lattice of the material due to the small current at a low sweeping rate. The active material is utilized sufficiently and Faradaic redox reaction occurs both on the surface and into the inner lattice of the $LiCoO_2$ material. On the contrary, no redox

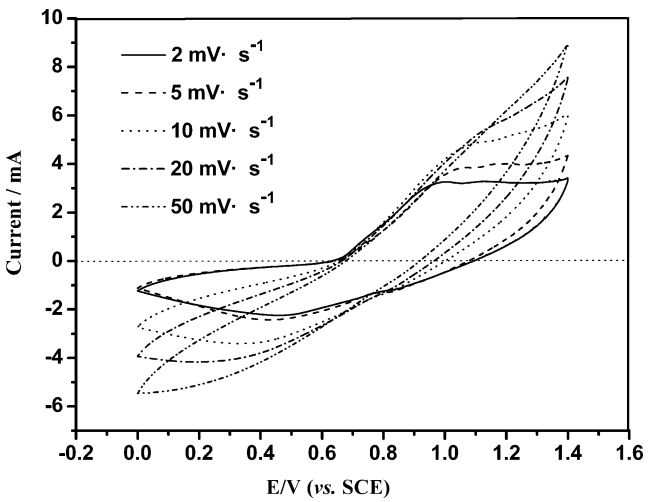

Fig. 3 CV curves of the $LiCoO_2$ electrode at various scan rates in 1 $molL^{-1}$ Li_2SO_4

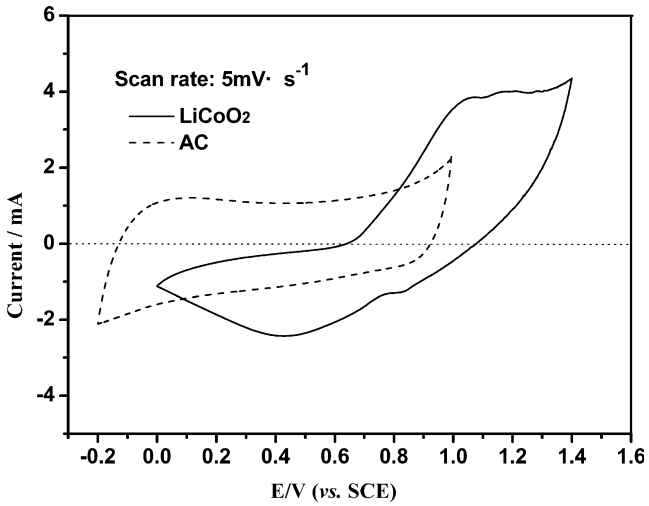

Fig. 5 CV curves of the $LiCoO_2$ and AC electrodes in 1 $molL^{-1}$ Li_2SO_4

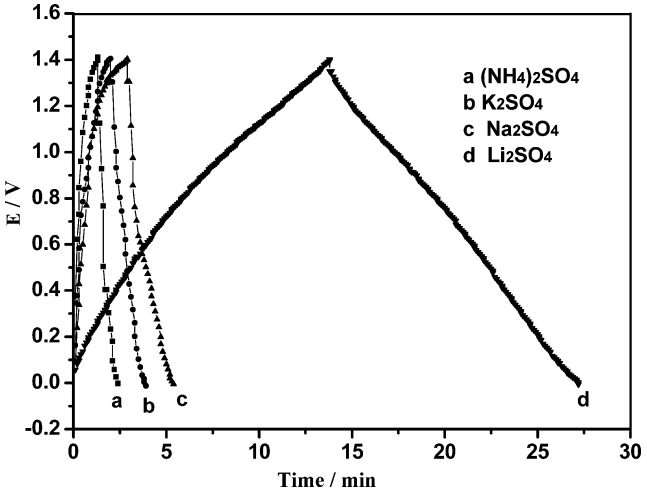

Fig. 6 The 20th cycle charge/discharge curves of the $LiCoO_2$/AC supercapacitor in various aqueous electrolytes

peaks occur when the sweeping rate is above 20 mVs^{-1}, revealing that the diffusion of Li-ions is almost limited to the surface of the $LiCoO_2$ particles due to the great current at high sweep rate. The active material is utilized insufficiently and Faradaic redox reaction occurs only on the surface of the electrode.

Figure 4 shows the CV curves of the AC electrode in various potential ranges in 1 $molL^{-1}$ Li_2SO_4 aqueous electrolyte. As shown in the figure, the AC electrode exhibits a rectangular shape curve in the potential range of –0.4–1.0 V (vs. SCE) in 1 $molL^{-1}$ Li_2SO_4 aqueous electrolyte, which is the typical character of double-layer capacitance.

As clearly shown in Fig. 5, there is no O_2 evolution peak on the $LiCoO_2$ electrode and H_2 evolution peak on the AC electrode in the potential range of 0–1.4 V, suggesting that the electrolyte remains stable in the potential window.

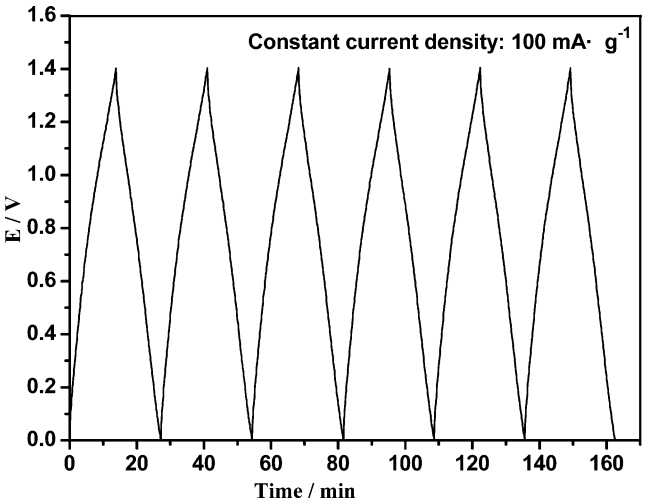

Fig. 7 Charge/discharge curves of the $LiCoO_2$/AC supercapacitor at a constant current density of 100 mAg^{-1} in 1 $molL^{-1}$ Li_2SO_4

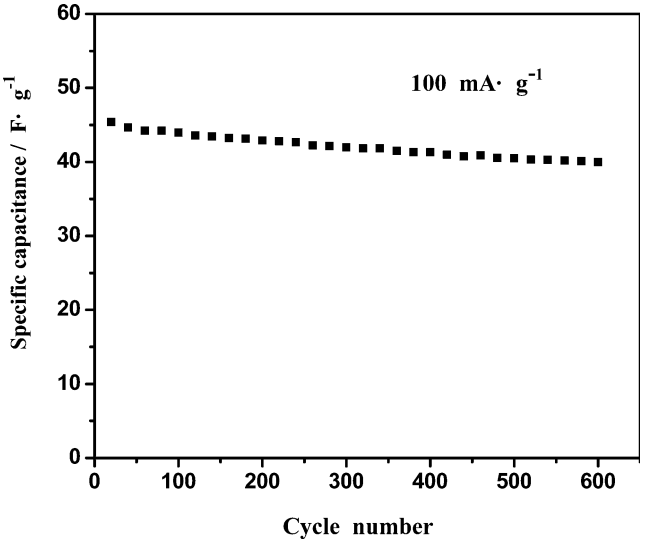

Fig. 8 Cycling performance of the $LiCoO_2$/AC supercapacitor at a constant current density of 100 mAg^{-1} in 1 $molL^{-1}$ Li_2SO_4

According to the "Results and discussion," the charge–discharge potential range of the $LiCoO_2$/AC supercapacitor is controlled between 0 and 1.4 V in 1 $molL^{-1}$ Li_2SO_4 solution.

Charge and discharge test

The influence of various aqueous solutions on the capacitive behavior of supercapacitor was investigated in order to find the most appropriate electrolyte. Figure 6 shows the 20th cycle charge–discharge curves of the supercapacitor in 1 $molL^{-1}$ Li_2SO_4, Na_2SO_4, K_2SO_4, and $(NH_4)_2SO_4$ solution. As can be seen in the figure, the $LiCoO_2$/AC capacitor exhibits much better capacitive behavior in 1 $molL^{-1}$ Li_2SO_4 solution than in the other solutions. The data show the charge storage mechanism of the $LiCoO_2$-positive electrode in the potential range of 0–1.4 V in aqueous electrolyte is associated with the insertion–deinsertion of Li-ion, which is similar to the charge storage mechanism of $LiCoO_2$ material in organic electrolyte. During the charge process, Li-ions in layered $LiCoO_2$ material were easily deinserted to form $Li_{1-x}CoO_2$, leading to many Li-ion vacant sites produced in the electrode material. During the discharge process, Li-ions in Li_2SO_4 solution could be easily reinserted into the vacant sites. However, it was very difficult for other cations (Na^+, K^+, and NH_4^+) to be inserted into the Li-ion vacant sites because their size did not match the size of the vacant sites. Even if a small amount of other cations were inserted into the $Li_{1-x}CoO_2$, the stability of the lattice structure would have seriously decreased. Therefore, the capacitive behavior of $LiCoO_2$/AC capacitor was worse in Na_2SO_4, K_2SO_4, and $(NH_4)_2SO_4$ solution. In the next experiments, Li_2SO_4 solution was chosen as the electrolyte of the $LiCoO_2$/AC supercapacitor.

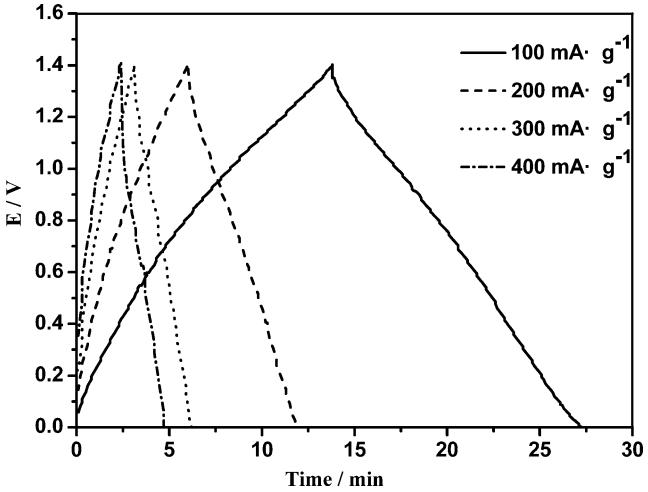

Fig. 9 Charge/discharge curves of the $LiCoO_2$/AC supercapacitor at various current densities in 1 $molL^{-1}$ Li_2SO_4

Based on the above discussion, the charge/discharge process can be described as follows:

$$LiCoO_2 = Li_{1-x}CoO_2 + x\,Li^+ + x e^- \quad (1)$$

$$AC + x Li^+ + x e^- = AC^{x-}//x Li(// : \text{electrical double layer}) \quad (2)$$

During the charge process, Li-ions are deinserted from the $LiCoO_2$-positive electrode, drifted into Li_2SO_4 electrolyte, and then transported to the AC-negative electrode to be adsorbed; on the contrary, during the discharge process, Li-ions are desorbed from the AC-negative electrode, drifted into Li_2SO_4 electrolyte, and then transported to the $LiCoO_2$-positive electrode to be inserted in. Li-ions transfer between the positive electrode and the negative electrode, and the concentration of Li-ions in Li_2SO_4 solution is approximately unchanged during the charge–discharge process.

Figures 7 and 8 show the charge–discharge curves and the cycling performance of the $LiCoO_2$/AC supercapacitor in 1 $molL^{-1}$ Li_2SO_4 solution at a constant current density of 100 mAg^{-1}. As shown in Fig. 7, the almost constant slope of the charge–discharge curves reveals that the $LiCoO_2$ electrode had high electrochemical reversibility and excellent capacitive characteristic.

Based on the discharge curves, the discharge specific capacitance (C) can be calculated as follows:

$$C = \frac{i \times \Delta t}{m \times \Delta V} \quad (3)$$

Where I (A), ΔV (V), Δt (s), and m are the discharge current density, discharge potential range, discharge time consumed in the potential range of ΔV, and the active mass of the two electrodes, respectively. According to the above equation, in the potential range of 0–1.4 V, the capacitor delivered a specific capacitance of 45.9 Fg^{-1} at the constant current density of 100 mAg^{-1} in 1 $molL^{-1}$ Li_2SO_4 solution. As can be observed in Fig. 8, the hybrid capacitor exhibited good capacity retention. The specific capacitance value remained 41.7 Fg^{-1} after 600 cycles.

As known to all, current density has great effect on the specific capacitance and cycling performance of supercapacitor. Figures 9 and 10 show the charge–discharge curves and cycling performance of the $LiCoO_2$/AC supercapacitor at various current densities in 1 $molL^{-1}$ Li_2SO_4, respectively. As can be seen in Figs. 9 and 10, the specific capacitance and cycling performance decrease with the increasing current densities. The $LiCoO_2$/AC capacitor had the greatest initial specific capacitance and the best cycling performance at the lowest current density of 100 mAg^{-1}. On the contrary, the capacitor had the smallest initial specific capacitance and the poorest cycling performance at the highest current density of 400 mAg^{-1}. The results were attributed to the storage energy mechanism of the $LiCoO_2$-positive electrode being associated with the insertion–deinsertion of Li-ions. When performing at a low current density, Li-ions could diffuse into the inner lattice of the $LiCoO_2$ material and the active mass could be fully utilized, so the supercapacitor delivered a relatively high specific capacitance; when performing at a high current density, it was difficult for Li-ions to diffuse into the inner lattice of the material, and the active mass was unable to be fully utilized, so the supercapacitor delivered a rather low specific capacitance. The results were in accordance with those obtained in cyclic voltammetry test.

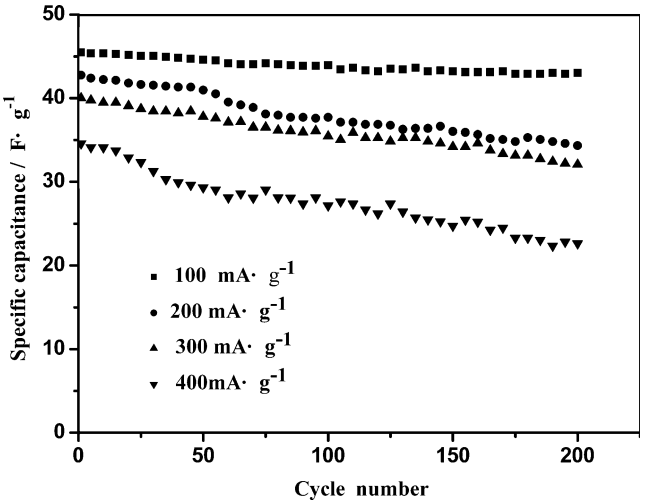

Fig. 10 Cycling performance of the $LiCoO_2$/AC supercapacitor at various current densities in 1 $molL^{-1}$ Li_2SO_4

Electrochemical impedance spectroscopy measurement

EIS was measured with a three-electrode system in which platinum foil and SCE were used as the counter and the reference electrode in various solutions. The frequency limits were set between 10 kHz to 0.01 Hz. Figure 11 shows the alternating current impedance spectra of the $LiCoO_2$ electrode before and after cycling in various aqueous solutions. As can be seen in Fig. 11, the resistance of the $LiCoO_2$ electrode is smaller in Li_2SO_4 than in the other aqueous solutions such as Na_2SO_4, K_2SO_4, and $(NH_4)_2SO_4$. During the charge–discharge process, Li-ions could easily diffuse between the $LiCoO_2$ material and electrolyte in Li_2SO_4 solution, so the resistance value was low. However, it was very difficult for the other cations (Na^+, K^+, and NH_4^+) to diffuse between the $LiCoO_2$ material and electrolyte, so the resistance value was high in these solutions. When a small amount of the other cations were inserted into the vacant sites, the stability of the lattice structure decreased seriously, so the resistance increased with the cycling numbers in Na_2SO_4, K_2SO_4, and $(NH_4)_2SO_4$ solution. The rather high resistance value would lead to rather poor electrochemical properties, so the pseudo-capacitive properties of the $LiCoO_2$/AC supercapacitor were much better in Li_2SO_4 than in Na_2SO_4, $K2SO_4$, and $(NH_4)_2SO_4$ solution, which supported the "Results and discussion" in the charge–discharge test.

Conclusion

The hybrid electrochemical capacitor was fabricated with $LiCoO_2$ as a positive electrode and AC as a negative electrode in various aqueous electrolytes. Its electrochemical properties were determined by cyclic voltammetry, charge–discharge test, and impedance spectroscopy measurement. The results showed that potential range, scan rate, species of aqueous electrolyte, and current density had great effect on the capacitive properties of the $LiCoO_2$/AC supercapacitor. The hybrid capacitor exhibited much better capacitive properties in 1 $molL^{-1}$ Li_2SO_4 than in other aqueous solutions such as 1 $molL^{-1}$ Na_2SO_4, K_2SO_4, and $(NH_4)_2SO_4$. This showed that the charge storage mechanism of the $LiCoO_2$-positive electrode was associated with Li-ions insertion–deinsertion in aqueous electrolyte. In the potential range of 0–1.4 V, the hybrid capacitor delivered a discharge specific capacitance of 45.9 Fg^{-1} (based on the active mass of the two electrodes) at 100 mAg^{-1} in 1 $molL^{-1}$ Li_2SO_4

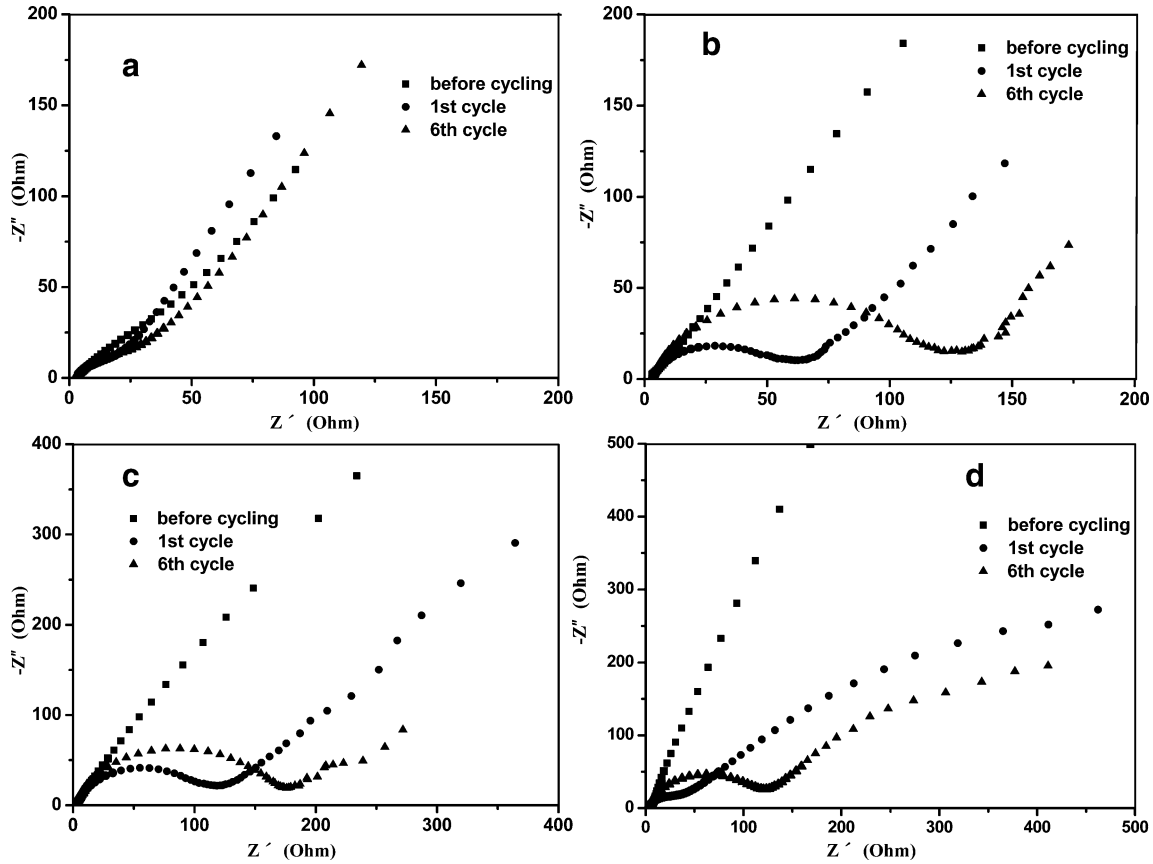

Fig. 11 The alternating current impedance spectra of the $LiCoO_2$ electrode before and after cycling in various aqueous electrolytes (**a** Li_2SO_4, **b** Na_2SO_4, **c** K_2SO_4 and **d** $(NH_4)_2SO_4$)

solution. The specific capacitance value remained 41.7 Fg^{-1} after 600 cycles. When current density increased, the specific capacitance decreased and the cycling performance became worse. The $LiCoO_2$/AC hybrid capacitor exhibited good pseudo-capacitance properties at current densities of 100–300 mAg^{-1} in 1 $molL^{-1}$ Li_2SO_4 solution.

References

1. Jeong YU, Manthiram A (2002) J Electrochem Soc 149:A1419–A1422
2. Zheng JP, Cygan PJ, Jow TR (1995) J Electrochem Soc 142:2699–2703
3. Hu Chi-Chang, Chen Wei-Chun, Chang Kuo-Hsin (2004) J Electrochem Soc 151:A281–A290
4. Jang Jong H, Kato Akiko, Machida Kenji, Naoi Katsuhiko (2006) J Electrochem Soc 153:A321–A328
5. Wang Xingyan, Wang Xianyou, Huang Weiguo (2005) J Power Sources 140:211–215
6. Subramanian V, Zhu Hongwei, Wei Bingqing (2006) J Power Sources 159:361–364
7. Broughton JN, Brett MJ (2005) Electrochimica Acta 50:4814–4819
8. Nam Kyung-Wan, Kim Kwang-Bum (2002) J Electrochem Soc 149:A346–A354
9. Lee Ji Yeong, Liang Kui, An Kay Hyeok, Lee YH (2005) Synthetic Metals 150:153–157
10. Wang Xing-Lei, He Kuan-Xin, Zhang Xiao-Gang (2006) Chin J of Inorg Chem 22:1019–1022
11. Kudo T, Ikeda Y, Watanabe T, Hibino M, Miyayama M, Abe H, Kajita K (2002) Solid State Ion 152–153:833–841
12. Pasquier Aurelien Du, Plitz Irene, Gural John, Menocal Serafin, Amatucci Glenn (2003) J Power Sources 113:62–71
13. Pasquier Aurelien Du, Laforgue Alexis, Simon Patrice (2004) J Power Sources 125:95–102
14. Chen Fang, Li Rengui, Hou Min, Liu Li, Wang Ran, Deng Zhenghua (2005) Electrochimica Acta 51:61–65
15. Huang Bai-Hui, Yang Ping, Zhang Bao-Hong, Shi Qing-Mo (2006) Chin J Power Sources 30:560–562
16. Yoshio Masaki, Tanaka Hirofumi, Tominaga Kenji, Noguchi Hideyuki (1992) J Power Sources 40:347–353
17. Myung ST, Kumagai N, Komaba S, Chung HT (2000) J of Appl Electrochem 30:1081–1085